SCIENTIFIC REPORTS

OPEN

SUBJECT AREAS:
ORAL DISEASES
VASCULAR DISEASES

Received
18 March 2014

Accepted
9 June 2014

Published
26 June 2014

Correspondence and requests for materials should be addressed to Y.-F.Z. (yifang@whu.edu.cn)

* These authors contributed equally to this work.

Disorganized vascular structures in sporadic venous malformations: a possible correlation with balancing effect between Tie2 and TGF-β

Gang Chen[1,2]*, Jian-Gang Ren[1]*, Wei Zhang[1], Yan-Fang Sun[1,2], Feng-Qin Wang[1], Rui-Fang Li[1], Jian Zhang[1] & Yi-Fang Zhao[1,2]

[1]The State Key Laboratory Breeding Base of Basic Science of Stomatology & Key Laboratory of Oral Biomedicine Ministry of Education, School & Hospital of Stomatology, Wuhan University, Wuhan, China, [2]Department of Oral and Maxillofacial Surgery, School & Hospital of Stomatology, Wuhan University, Wuhan, China.

Venous malformations (VMs) are among the most common slow-flow vascular malformations characterized by irregular venous channels, luminal thrombi, and phleboliths. To systematically manifest the disorganized vascular structures in sporadic VMs, we initially evaluated histopathological characteristics, perivascular cell coverage, adhesion molecules expression and vascular ultrastructures. Then, the expression of Tie2 and TGF-β in VMs was detected. Meanwhile, the *in vitro* studies were performed for mechanism investigation. Our data showed that the perivascular α-SMA$^+$ cell coverage and expression of adhesion molecules in VMs were significantly decreased compared with those in the normal skin tissues. We also found that the expression and phosphorylation levels of Tie2 were upregulated, whereas TGF-β was downregulated in VMs, and they were negatively correlated. Moreover, the *in vitro* results also revealed a possible balancing effect between Tie2 and TGF-β, as demonstrated by the findings that Ang-1 (agonist of Tie2) treatment significantly downregulated TGF-β expression, and treatment with recombinant TGF-β could also suppress Tie2 expression and phosphorylation. This study provided strong evidence supporting the disorganized vascular structures and dysregulation of related molecules in sporadic VMs, and demonstrated a possible balancing effect between Tie2 and TGF-β, which might help to develop novel therapeutics for vascular disorganization-related disorders.

Vascular malformations, which are composed of abnormal vasculature[1], are generally categorized as slow- and fast-flow lesions in terms of vessel morphology and flow speed[2]. Venous malformations (VMs) are among the most common slow-flow vascular malformations, accounting for approximately one-half to two-thirds of vascular malformations[3]. VMs are mainly presented at birth with a reported incidence of 1–2 per 10,000 births and a prevalence of 1%[4].

VMs frequently occur in the oral and facial regions and may continue to grow throughout a patient's lifetime[5]. Furthermore, VMs are characterized by thin-walled and dilated sponge-like channels, luminal thrombi and phleboliths[6]. VMs may also be associated with several types of syndromes, such as Klippel Trenaunay syndrome and Blue Rubber Bleb Nevus syndrome[5]. VMs often disrupt the physiological functions of adjacent normal tissues, including the muscles[7], bones[8] and nerves[9,10]. In addition to physiological illness, the patients with VMs have to suffer from enormous mental pressure caused by deformation of facial appearance, which dramatically decreases their life quality[11]. Therefore, it is important to dig deeper into the pathogenesis of this disease, which may help to develop new strategies of therapeutics.

It is well known that dilated venous channels and disorganized vascular smooth muscle cell (vSMC) layer are frequent phenomenons in VMs[1,12]. However, close attentions and deeper researches on these phenomenons are scarce. Tie2 is the receptor of angiopoietin-1 (Ang-1), Ang-2, Ang-3 (in mouse) and Ang-4 (in human)[13,14]. Currently, the mutation of *TEK, the* coding gene of Tie2, has been implicated in the development of inherited VMs. *TEK* mutation can result in the constitutive activation of Tie2 independent of the corresponding ligands[15–17]. Nevertheless, the expression level and activation status of Tie2 in sporadic VMs as well as the possible pathological significance are still to be clarified.

In the present study, the disorganized vascular structures in sporadic VMs were systematically manifested at cellular and molecular levels. Meanwhile, we showed the negatively correlated Tie2 overactivation and transforming growth factor-beta (TGF-β) suppression in VM tissues. Importantly, by employing corresponding agonist and recombinant factor, we also revealed a possible balancing effect between the Tie2 and TGF-β pathways in endothelial cells (ECs), and indicated its potential significance in vascular regulation.

Results

Perivascular α-SMA$^+$ cell coverage in VMs was significantly decreased. To investigate in depth the pathological changes in the blood vessels associated with VMs, we first analyzed the vascular morphology as well as the presence and distribution of perivascular cells by double-labelling immunofluorescence using anti-CD34 and anti-α-SMA antibodies. As shown in Figure 1A, VMs were composed of irregular venous-type channels, which were varied in size and lined by flat discontinuous endothelium. Moreover, the perivascular α-SMA$^+$ cells (pericyte and smooth muscle cell) in VM tissues were randomly distributed and focally scant or even absent. The quantified results revealed that the immunofluorescence intensity of α-SMA in VM tissues was evidently weaker than that in normal skin (SK) tissues.

CD34 and α-SMA (Figure 1B) in VM and control tissues, including SK, pyogenic granulomas (PG) and placenta (PL), were then subjected to immunohistochemical double-staining to determine whether or not the distribution of perivascular α-SMA$^+$ cells in VMs was distinctive. The quantified data showed that the perivascular α-SMA$^+$ cell coverage in VMs was significantly decreased compared with that in the SK tissues (Figure 1C). The perivascular α-SMA$^+$ cells in the SK tissues were densely and uniformly distributed. In PG and PL tissues, the perivascular α-SMA$^+$ cell coverage was the lowest as a result of neovasculature.

Changes in the vascular ultrastructure in VMs. To further investigate the characteristics of blood vessels in VMs, we performed transmission electron microscopy (TEM) and obtained the ultrastructures. Figure 2A showed that the blood vessels in SK tissues are closely surrounded by vSMCs and exhibit extensive, tight junctions between adjacent ECs. By contrast, poor junctions and a tortuous stretched abluminal surface were found between adjacent ECs in VMs. Poor or no contact between adjacent SMCs was also detected in VMs (Figure 2B) and the basement membrane (BM) was imcomplete or even absent. Moreover, the intima of blood vessels in VMs was mainly lined with discontinuous and apertured ECs (Figure 2C).

Expression levels of adhesion molecules were downregulated in VMs. VE-Cadherin and N-Cadherin are essential adhesion molecules involved in intercellular contact, and their expressions are associated with the organization of vascular structures[18,19].

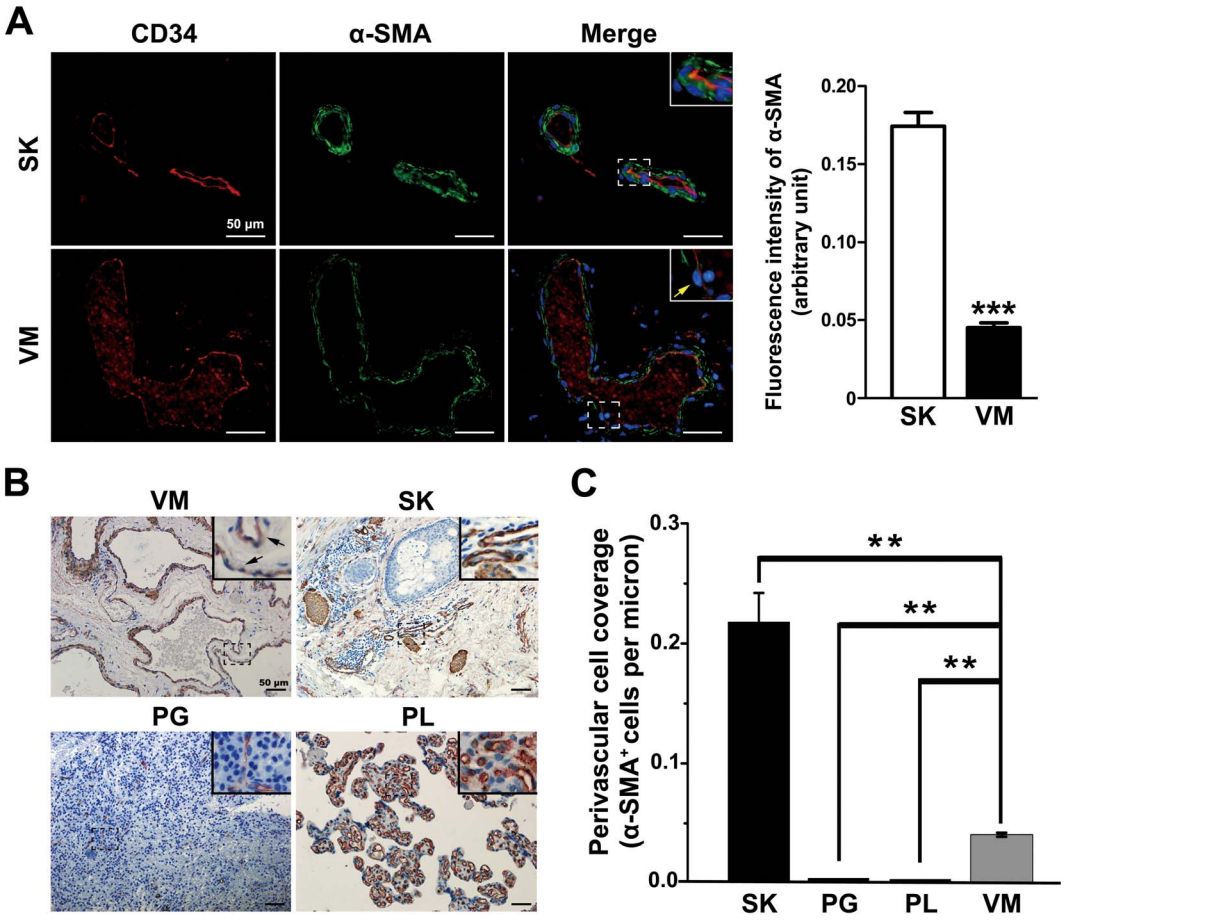

Figure 1 | Detection and evaluation of perivascular α-SMA$^+$ cell coverage in venous malformations (VMs). (A) Double-labelling immunofluorescence for CD34 and α-SMA in VM and normal skin (SK) tissues. The fluorescence intensity of perivascular α-SMA is significantly decreased in VMs compared with that in the SK tissues. Nuclei are counterstained with Hoechst. (B) Double-labelling immunohistochemistry for CD34 and α-SMA in VM, SK, pyogenic granulomas (PG) and placenta (PL) tissues. The arrows in the magnified images of (A) and (B) indicate the areas without vSMCs in VMs. (C) Quantification of perivascular α-SMA$^+$ cell coverage in VM, SK, PG and PL tissues. Data are expressed as means ± SEM. **, $P < 0.01$ versus VM tissues.

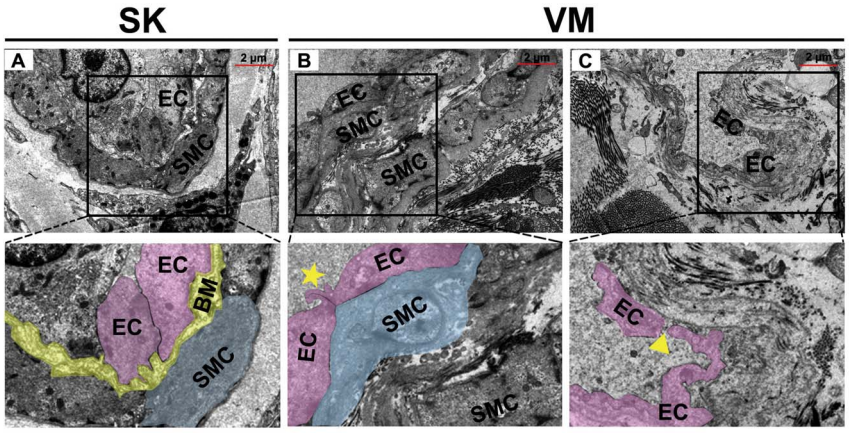

Figure 2 | Changes in the vascular ultrastructure in venous malformations (VMs). (A) In normal skin (SK) tissues, the blood vessels are closely surrounded by SMCs and extensive tight junctions are present between adjacent ECs. (B) By contrast, poor junctions and a tortuous stretched abluminal surface between adjacent ECs in VMs are detected (asterisk). (C) The intima of blood vessels in VMs is mainly lined with discontinuous and apertured ECs (triangle). EC: endothelial cells; SMC: smooth muscle cells; BM: basement membrane.

Thus, we evaluated the expression levels of VE-Cadherin and N-Cadherin in VMs by immunohistochemistry and real-time qPCR, respectively. Our data revealed that both VE-Cadherin and N-Cadherin in SK tissues were strongly expressed around the blood vessels. However, their immunoreactivities were down-regulated in VM tissues (Figure 3A and 3C). Real-time qPCR results demonstrated the decreased mRNA expression levels of VE-Cadherin and N-Cadherin in VM tissues compared with the SK tissues (Figure 3B and 3D).

Expression and phosphorylation levels of Tie2 were upregulated in VMs. Previous studies have reported that VM-causative mutant forms of *TEK* increase the phosphorylation level of Tie2 when expressed in cells[17,20]. To examine the activation status of Tie2 in sporadic VM tissues, we detected the expression and phosphorylation levels of Tie2 in 29 VMs patients without family history. The patients' information was indicated in Table 1. The representative images of Tie2 and p-Tie2 immunostaining are shown in Figure 4A and 4C, respectively. It was found that Tie2 and p-Tie2

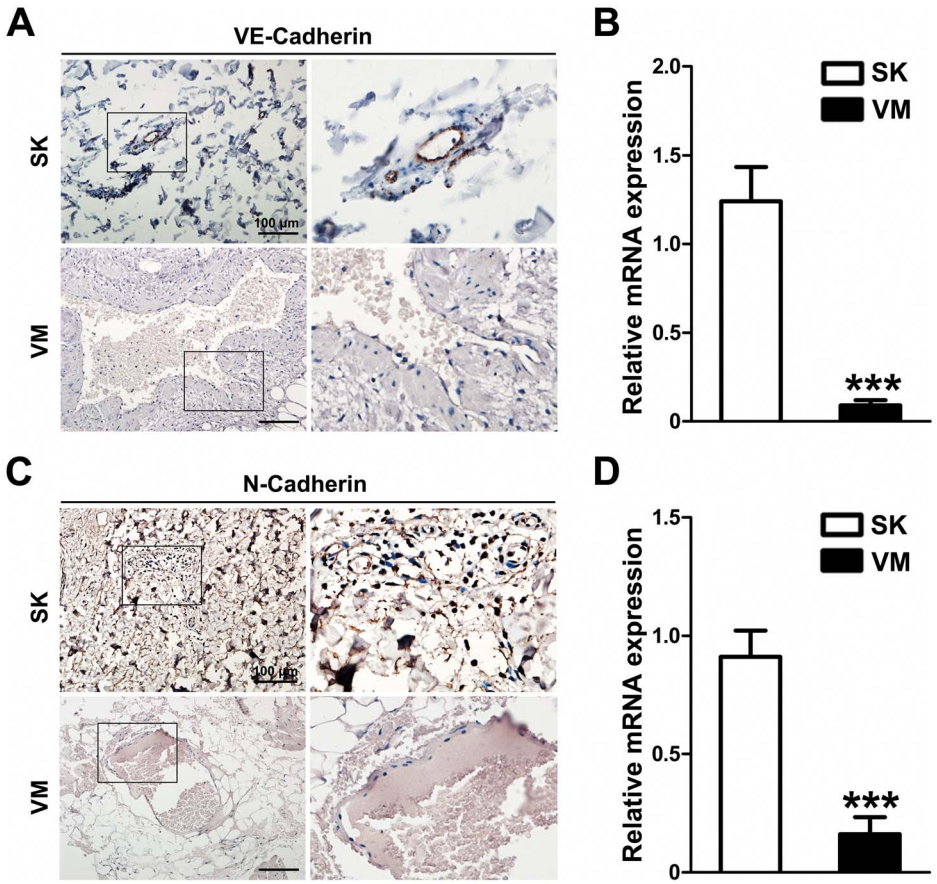

Figure 3 | Immunohistochemistry and real-time qPCR analyses of adhesion molecule expression in venous malformations (VMs). (A, C) In normal skin (SK) tissues, VE-Cadherin and N-Cadherin are strongly expressed around the blood vessels. However, their expression levels are remarkably downregulated in VM tissues. (B, D) Quantification of the mRNA expression levels of VE-Cadherin and N-Cadherin in VM and SK tissues. Data are expressed as means ± SD for qPCR. ***, $P < 0.001$ versus SK tissues.

Table 1 | Summary of clinical features of venous malformations patients

Patient NO.	Gender	Age (years)	Location	Therapy
1	M	48	Lower Lip	NO
2	M	18	Zygomatic Area	NO
3	M	34	Tongue	NO
4	M	21	Tongue	NO
5	M	25	Left Ear	NO
6	M	16	Right Cheek	NO
7	F	39	Tongue	NO
8	F	1	Submandibular Area	NO
9	F	13	Upper Lip	NO
10	F	40	Lower Lip	NO
11	F	39	Left Cheek	NO
12	F	79	Right Cheek	NO
13	M	64	Tongue	NO
14	F	25	Tongue	NO
15	M	63	Submandibular Gland	NO
16	M	14	Parotid Gland	NO
17	F	24	Cheek	NO
18	F	47	Right palatine	NO
19	F	9	Submandibular Area	NO
20	M	40	Parotid Gland	NO
21	F	18	Tongue	NO
22	M	48	Tongue	NO
23	F	14	Parotid Gland	NO
24	M	23	Facial Deep Region	NO
25	F	54	Oral Floor	NO
26	F	74	Right Cheek	NO
27	F	55	Tongue	NO
28	M	3	Left Cheek	NO
29	F	42	Zygomatic Area	NO

Abbreviations: M, male; F, female.

were strongly expressed in the blood vessels of VMs. The quantified results showed that the immunoreactivities of Tie2 and p-Tie2 were significantly upregulated in VM tissues compared with those in SK tissues (Figure 4B and 4D), which suggested the elevated expression and phosphorylation of Tie2 in sporadic VMs. The results of serial immunohistochemistry and double-labeling immunofluorescence further indicated that Tie2 phosphorylation was negatively correlated with α-SMA$^+$ cell coverage. In particular, specific areas characterized by high Tie2 phosphorylation coinciding with few α-SMA$^+$ cells were observed (Figure 5). Spearman rank test also demonstrated that the overactivation of Tie2 was closely related to the decreased perivascular α-SMA$^+$ cell coverage in VMs (Figure 6A), which further indicated the potential significance of Tie2 in the regulation of vascular structures.

Expression level of TGF-β was downregulated in VMs. TGF-β production in ECs plays a critical role in perivascular SMC migration and differentiation[21,22]. Thus, we investigated the expression level of TGF-β in VMs, and whether it contributes to the disorganized vascular structures in VMs. Figure 7A showed that TGF-β was extensively expressed in ECs, SMCs and other cells in SK tissues. By contrast, the TGF-β expression level was significantly downregulated in VMs (Figure 7A and 7B) ($P < 0.001$). Real-time qPCR results also showed that the mRNA expression level of TGF-β was evidently decreased in VM tissues compared with that in SK tissues (Figure 7C). In addition, the downregulation of TGF-β was closely associated with the decrease in perivascular α-SMA$^+$ cell coverage (Figure 6B).

Tie2 activation was negatively correlated with TGF-β expression in VMs. The above results have showed that both Tie2 overactivation and TGF-β down-regulation were associated with the decreased perivascular α-SMA$^+$ cell coverage in VMs. Therefore, we doubted whether or not a correlation could be observed between the changes in these two signals. As expected, the double-labelling immunofluorescence results revealed a synchronous but reversed change in Tie2 and TGF-β in VM tissues. This result indicated that these two molecules were negatively correlated with each other (Figure 8A, 8B and 8C). Spearman rank test also demonstrated that p-Tie2 upregulation was significantly correlated with TGF-β downregulation in VM tissues (Figure 8D). To verify these findings, we investigated the expression levels of Tie2, p-Tie2 and TGF-β in venous malformation ECs (VMECs) by conducting double-immunofluorescence analysis of cells. As shown in Figure 9, the cultured VMECs exhibited cobblestone morphology under phase-contrast microscope. In addition, the immunofluorescence staining for specific markers of endothelial cells (e.g. CD31, VE-Cadherin, VIII Factor, and VEGFR-2) was positive. Figure 10A, 10B and 10C showed that the expression levels of the total-Tie2 and p-Tie2 were evidently upregulated in VMECs; by contrast, the TGF-β expression level was significantly decreased compared with that in HUVECs. Using Tie2 agonist Ang-1 and recombinant TGF-β, we also determined a possible balancing effect between Tie2 and TGF-β pathways in ECs. The results showed that Ang-1 treatment significantly downregulated the expression of TGF-β and its downstream signal p-Smad3, and treatment with recombinant TGF-β could also suppress the expression and phosphorylation of Tie2 (Figure 10D and 10E).

Discussion

VMs are among the most frequent slow-flow vascular malformations observed in the oral maxillofacial regions[3]. VMs have been previously linked to dilated channels with sparse vascular smooth muscle cells, which suggested the existence of disorganized vascular structures[12,16]. In the present study, these disorganized vascular structures were systematically manifested in sporadic VMs in terms of histopathological characteristics, perivascular cell coverage, adhesion molecules expression and vascular ultrastructures. Our data showed that most of the vessels in VMs were remarkably enlarged and irregular. We also found that the perivascular α-SMA$^+$ cell coverage was significantly decreased in VMs compared with that in the SK tissues. Moreover, the expression levels of intercellular adhesion molecules were significantly downregulated in VMs. Several abnormal vascular ultrastructures were also detected. These results provided additional and strong evidence revealing the disorganized vascular structures in VMs.

According to the embryonic development theory and current studies, the vessels without enough supporting perivascular cells cannot be retained for a long time and may tend to regress spontaneously[23]. Nevertheless, such disorganized vessels can survive in VMs, but the exact mechanism remains unknown. *TEK* mutation in ECs can significantly increase the autophosphorylation of Tie2[17,20]. As a consequence, PI3K/Akt pathway is activated and EC apoptosis is inhibited[24,25]. This result may be implicated in the development of inherited VMs. However, these findings cannot elucidate other relevant issues, such as the expression level and activation status of Tie2 in sporadic VMs. These results also failed to determine whether or not the increased Tie2 phosphorylation is related to the disorganized vascular structures in VMs. To examine these conditions, we analyzed the expression and phosphorylation levels of Tie2 in sporadic 29 VMs. The immunohistochemical results indicated that the expression and phosphorylation levels of Tie2 were significantly increased in the tested samples. Moreover, the upregulation of Tie2 phosphorylation was closely correlated with the decreased perivascular α-SMA$^+$ cell coverage.

The recruitment of perivascular SMCs and interaction between ECs and SMCs exhibit important functions in vascular formation[21]. TGF-β is also essential for SMC migration, differentiation, and vascular stabilization[21,22]. Thus, we investigated whether or not TGF-β

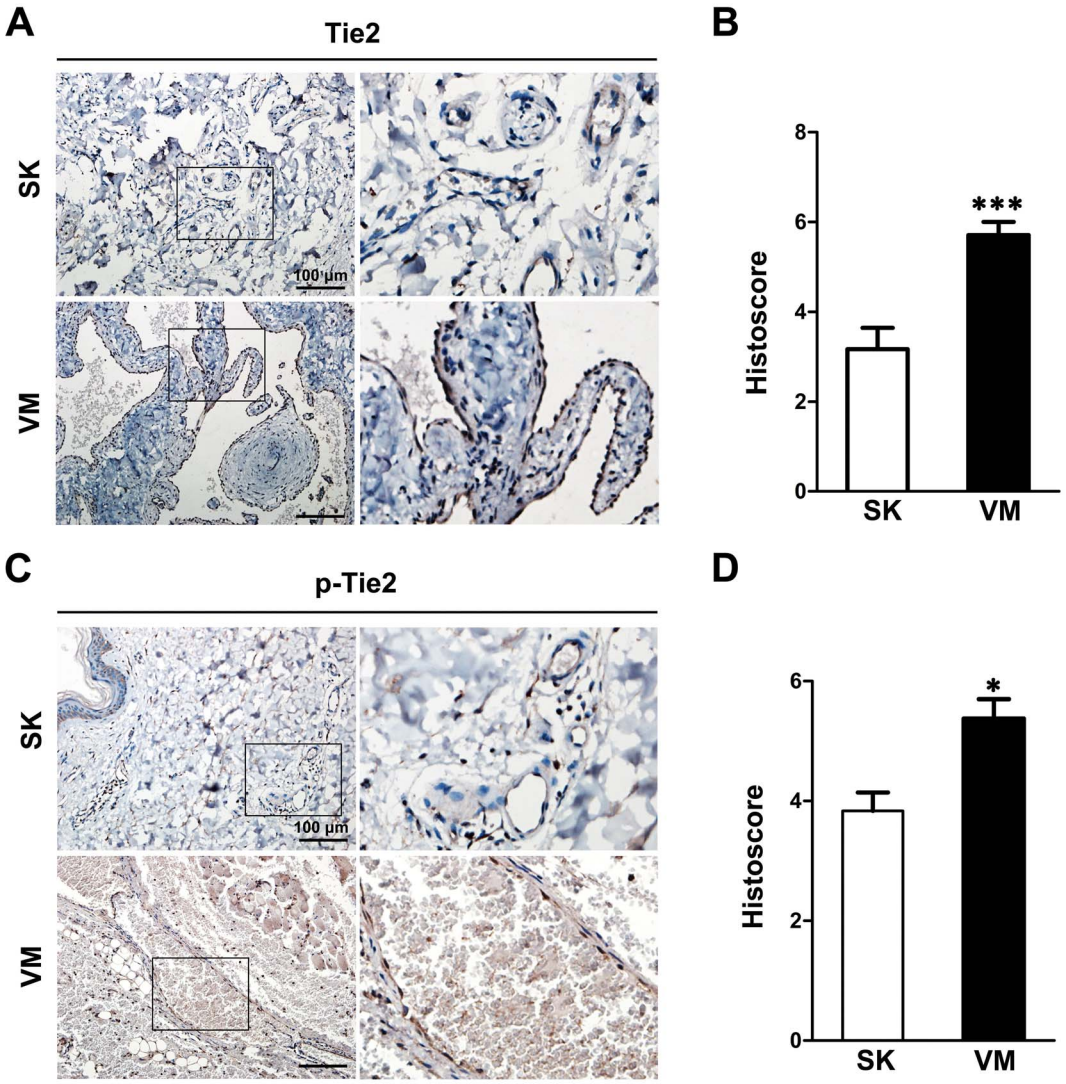

Figure 4 | Immunohistochemical staining to detect Tie2 expression and phosphorylation in venous malformations (VMs). (A, C) Increased expression and phosphorylation of Tie2 are observed in VM tissues when compared with normal skin (SK) tissues. (B, D) Quantification of the expression and phosphorylation levels of Tie2 in VM and SK tissues. Data are expressed as means ± SEM. *, $P < 0.05$; ***, $P < 0.001$ versus SK tissues.

signalling is involved in the disorganized vascular structures in VMs by evaluating the TGF-β expression level in VMs. The results showed that both the immunoreactivity and the mRNA expression level of TGF-β were significantly decreased in VMs compared with those in the SK tissues. We also found that TGF-β expression was negatively correlated with Tie2 phosphorylation. We further observed Ang-1 treatment significantly downregulated TGF-β expression and the corresponding downstream signal. Conversely, the treatment with recombinant TGF-β could also suppress the expression and phosphorylation of Tie2. Therefore, a possible balancing effect might exist between Tie2 and TGF-β signalling pathways in ECs. These results suggested that a balancing effect and alternative selection may be determined between self-survival and organization for the blood vessels in VMs. In particular, increased Tie2 expression and phosphorylation may enhance the survival ability and prevent the apoptosis of ECs. This increased expression and phosphorylation may simultaneously suppress TGF-β expression, impede vascular organization, and result in the persistent existence of disorganized vascular structures in VMs. Nevertheless, further investigation is still needed to determine the precise mechanisms underlying the interaction between Tie2 and TGF-β signalling pathways.

In summary, our present study provided strong evidence supporting the disorganized vascular structures and dysregulation of related molecules in sporadic VMs. This study also demonstrated a possible balancing effect between Tie2 and TGF-β in ECs. Our results shed new light on the possible pathogenesis of VMs, and might help to develop novel therapeutic strategies for vascular disorganization-related disorders, such as vascular malformations and tumor angiogenesis.

Methods

Tissue samples and immunohistochemistry. Twenty-nine samples of venous malformations without treatment history, 9 samples of pyogenic granulomas, 4 samples of placentas, as well as 6 samples of healthy donor skin were collected at Hospital of Stomatology, Wuhan University. All the specimens were fixed in buffered 4% paraformaldehyde and embedded in paraffin, and the procedures were performed according to the National Institutes of Health guidelines regarding the use of human tissues. This study was approved by the review board of the Ethics Committee of Hospital of Stomatology, Wuhan University. The immunohistochemical analysis was performed according to our earlier procedures[26,27]. Briefly, the serial tissue sections were dewaxed in xylene, rehydrated in a graded series of ethanol and double-distilled water, and antigen retrieved by high pressure. Then the sections were washed with PBS and incubated within 3% hydrogen peroxide and 10% goat serum for 15 min. After that the slides were incubated overnight at 4°C with TGF-β (ABclonal), VE-Cadherin (Epitomics), N-Cadherin (Santa Cruz), Tie2 (ABclonal) and phosphorylated Tie2 (Abnova). The antibody binding was then detected by horseradish peroxidase-conjugated secondary antibody using diaminobenzidine substrate kit (Dako). For evaluation of immunohistochemical staining, at least five fields with typical pathological changes characterized by thin-walled dilated sponge-

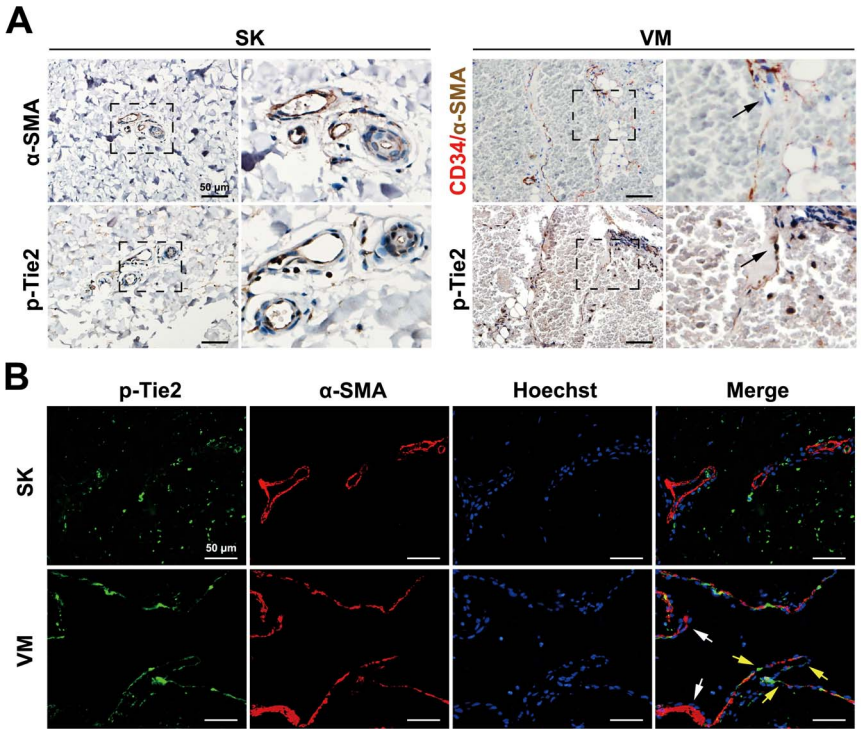

Figure 5 | The serial sections and double-labeling immunofluorescence for p-Tie2 and α-SMA in venous malformations (VMs). The black and yellow arrows showed the specific areas characterized by high p-Tie2 coinciding with low α-SMA, while the white arrows indicated the areas with low p-Tie2 and high α-SMA in VMs.

like vessels in VM tissues were randomly selected at a magnification of 200 with light microscope (Leica) and counted by two independent observers. All the inter- and intra-observer agreement was over 65% with Kappa values of over 0.41 to ensure the reliability of data. Meanwhile, normal veins characterized by dense and uniform perivascular α-SMA$^+$ cells in normal skin tissues were selected as controls. The staining scores were calculated as the summation of staining intensity (0, negative, no staining; 1, faint yellow, mild staining; 2, claybank, moderate staining; and 3, brown, intense staining) and the percentage of cells showing positive cytoplasmic or membrane staining (0, <10%; 1, 10%–25%; 2, 25%–50%; 3, 50–75%; and 4, 75–100% of endothelial cells).

Transmission electron microscopy. For transmission electron microscopy (TEM), fresh specimens of normal skin and VMs were immediately fixed in 2.5% glutaraldehyde for 3 h at room temperature and then stored at 4°C. When used, the specimens were postfixed in 1% osmium tetroxide with 0.1% potassium ferricyanide, dehydrated through a graded series of ethanol (30–90%), and embedded in Epon. Ultrathin sections (65 nm) were cut, stained with 2% uranyl acetate and Reynold's lead citrate and examined using a FEI Teenai G^2 20 Twin Transmission Electron Microscope.

Double-labeling immunohistochemistry. In brief, paraffin embedded specimens were cut into 4-μm sections, deparafinized, antigen retrieved by high pressure, and then incubated overnight with anti-CD34 antibody (1 : 200), followed by secondary goat anti-mouse biotinylated antibody, and then incubated with hydrogen peroxidase-labelled detection system for 20 min. Peroxidase reaction was performed using 3-amino-9-ethylcarbazole, resulting in an overwhelming red of the membrane. After that, sections were incubated with anti-α-SMA antibody at a dilution of 1 : 400 for 60 min, followed by secondary goat anti-rabbit biotinylated antibody, and then incubated with hydrogen peroxidase-labelled detection system for 20 min. Peroxidase reaction was performed using diaminobenzidine, resulting in a dark sepia cytoplasm staining. For analysis of the perivascular cell coverage, α-SMA positive cells at magnification of 200 in five random fields were counted blindly by two investigators, and then the number of α-SMA positive cells per vessel length was determined using Photoshop CS5.

Double-labeling immunofluorescence. Briefly, the tissue sections of paraffin-embedded specimens were dewaxed in xylene, rehydrated in a graded series of ethanol and double-distilled water. The antigen retrieval was performed by using high pressure. After that, endogenous peroxidase of slices was blocked by incubation in 3%

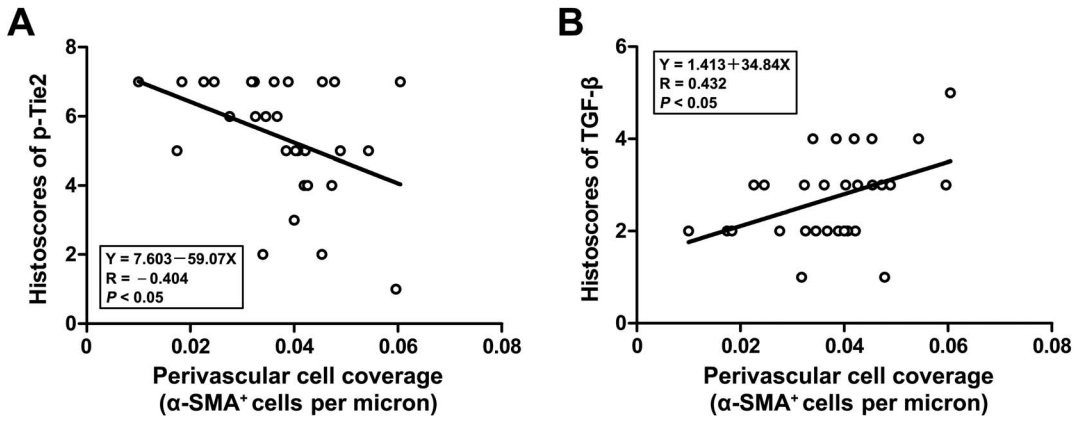

Figure 6 | Spearman rank correlation analyses for the immunostainings of tested markers in venous malformations (VMs). (A) The phosphorylation level of Tie2 was negatively correlated with perivascular α-SMA+ cell coverage. (B) TGF-β expression showed significantly positive correlation with perivascular α-SMA+ cell coverage in VMs.

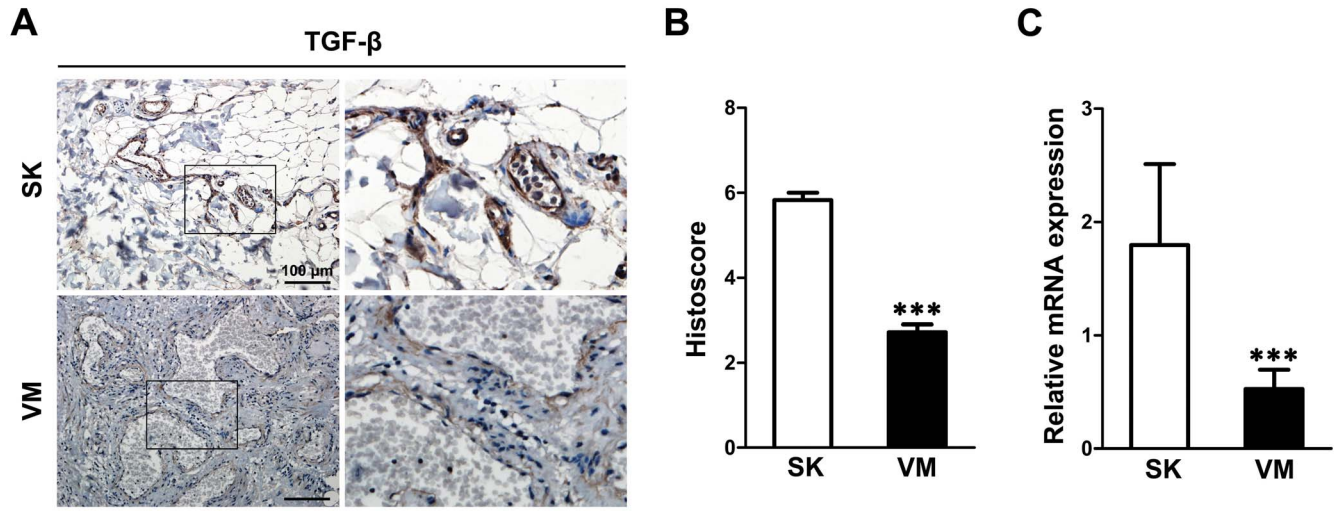

Figure 7 | Immunohistochemistry and real-time qPCR analyses to determine TGF-β expression in venous malformations (VMs). (A) TGF-β is downregulated in VM tissues when compared with normal skin (SK) tissues. (B) Quantification of TGF-β immunoreactivity in VM and SK tissues. (C) Quantification of the mRNA expression level of TGF-β in VM and SK tissues. Data are expressed as means ± SEM for histoscore and means ± SD for qPCR. ***, $P < 0.001$ versus SK tissues.

bovine serum albumin (Sigma) for 1 h at room temperature. The sections were then incubated with mouse anti-human CD34 (1 : 100) and rabbit anti-human α-SMA (1 : 200) together overnight at 4°C. After washing with PBS, the sections were sequentially incubated with Dylight488 goat anti-mouse antibody and Dylight549 goat anti-rabbit antibody (EarthOx) for 1 h, respectively. Nuclei were counterstained with Hoechst, followed by observation and quantification under a fluorescence microscope (Leica).

Cell culture. The method for culturing primary VM endothelial cells (VMECs) was summarized as follows: Specimens of venous malformation were obtained from the Hospital of Stomatology, Wuhan University that was approved by the review board of the Ethics Committee of the Wuhan University Hospital of Stomatology. The tissue was digested with 0.2% collagenase A (Roche Diagnostics, Indianapolis, IN) in Dulbecco modified Eagle medium (Invitrogen, Carlsbad, CA) supplemented with 2% FBS and PSF (Gibco) for 1 hour at 37°C. The tissue homogenate were filtered through

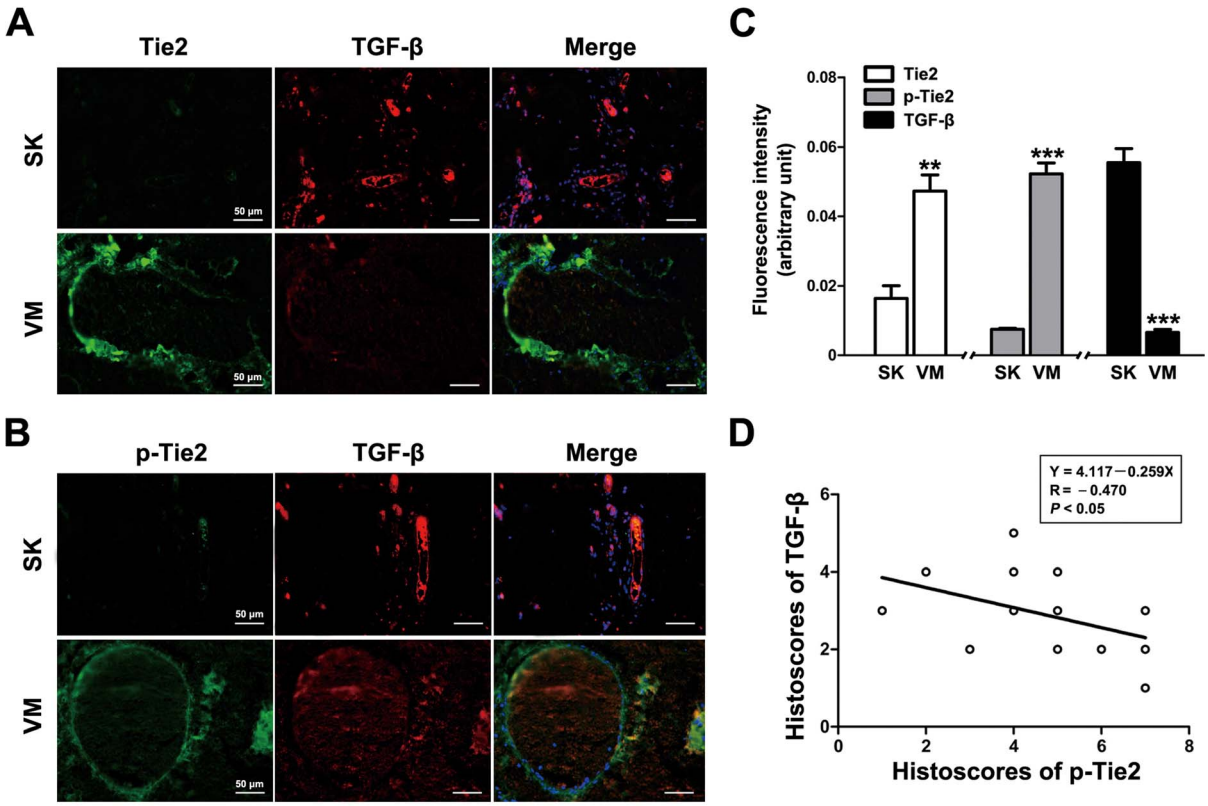

Figure 8 | Negative correlation between Tie2 and TGF-β in venous malformations (VMs). (A, B) Immunofluorescence staining for Tie2, p-Tie2 and TGF-β in VMs and normal skin (SK) tissues. Nuclei are counterstained with Hoechst. (C) The fluorescence intensities of Tie2 and p-Tie2 are significantly increased in VMs compared with SK tissues; by contrast, the fluorescence intensity of TGF-β is decreased. (D) Spearman rank correlation test reveals a negative correlation between p-Tie2 upregulation and TGF-β downregulation in VMs. Data are expressed as means ± SEM. **, $P < 0.01$; ***, $P < 0.001$ versus SK tissues.

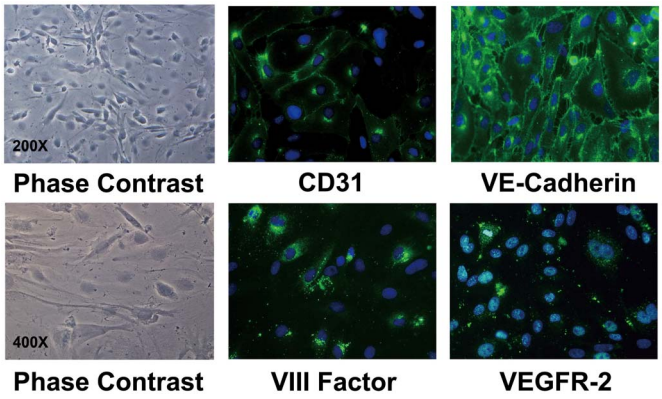

Figure 9 | Culture and identification of VMECs. VMECs exhibited cobblestone morphology under phase-contrast microscope. In addition, the immunofluorescence staining for specific markers of endothelial cells (e.g. CD31, VE-Cadherin, VIII Factor, and VEGFR-2) was positive.

a 70-μm cell strainer (BD). Red blood cells were lysed by incubating the sample in NH_4Cl for 10 minutes on ice. Cells were filtered through a 40-μm strainer to obtain a single-cell suspension form which the cells expressing the endothelial cell antigen CD31 were selected. $CD31^+$ and $CD31^-$ cells were isolated using anti-CD31-coated magnetic beads (Miltenyi Biotec, Auburn, CA) and cultured separately on fibronectin (1 μg/cm^2) coated plates with Endothelial Culture Medium (ECM) that was supplemented with 20% FBS, SingleQuot (ScienCell), and PSF. Human umbilical vein endothelial cells (HUVECs) were isolated from human umbilical cord veins by collagenase treatment as described previously[28], and were cultured in Endothelial Basal Medium (Cambrex Bio Science, Walkersville, MD) supplemented with 20% fetal bovine serum, SingleQuot (Cambrex Bio Science), and PSF. When cells were grown to 70% confluence, they were treated with human recombinant TGF-β (20 ng/ml) or Ang-1 (50 ng/ml) in Endothelial Basal Medium containing 5% fetal bovine serum and further cultured for 24 h.

Real-time quantitative PCR. Isolation of total RNA, synthesis of cDNA, and real-time quantitative PCR (qPCR) were performed according to our previous study[27]. Briefly, total RNA was isolated with TRIzol Reagent (Invitrogen), and aliquots (1 μg) of RNA were reverse transcribed to cDNA (20 μl) with oligo(dT) and M-MuLV reverse transcriptase (Fermentas, Glen Burnie, MD). Then one-fifth of the cDNA was used as a template for PCR using SYBR Premix Ex TaqTM (Perfect Real Time) kits (Takara, Kyoto, Japan) in an ABI 7500 Real-Time PCR System (Applied Biosystems, Foster City, CA). 18s rRNA was chosen as an internal control. The primer nucleotide sequences for PCR are presented in Table 2.

Western blot analysis. The western blot analysis was carried out according to our previous description[29,30]. In brief, the proteins in corresponding cells were extracted, and the protein concentration was estimated using BCA assay (Pierce Chemical, Rockford, IL). Subsequently, an aliquot of 40 μg protein of each sample was separated on 10% SDS-polyacrylamide gels and electroblotted on polyvinylidene fluoride membranes (Roche Applied Science, Germany). Then the blots were then blocked overnight with 5% skimmed milk and further probed with primary antibodies at dilutions recommended by the suppliers. After that, the immunoblots were detected using a chemiluminescence kit (Pierce).

Statistical analysis. Student's *t*-test and Spearman rank correlation test were used for statistical analysis. For the comparisons, $P < 0.05$ was considered statistically significant.

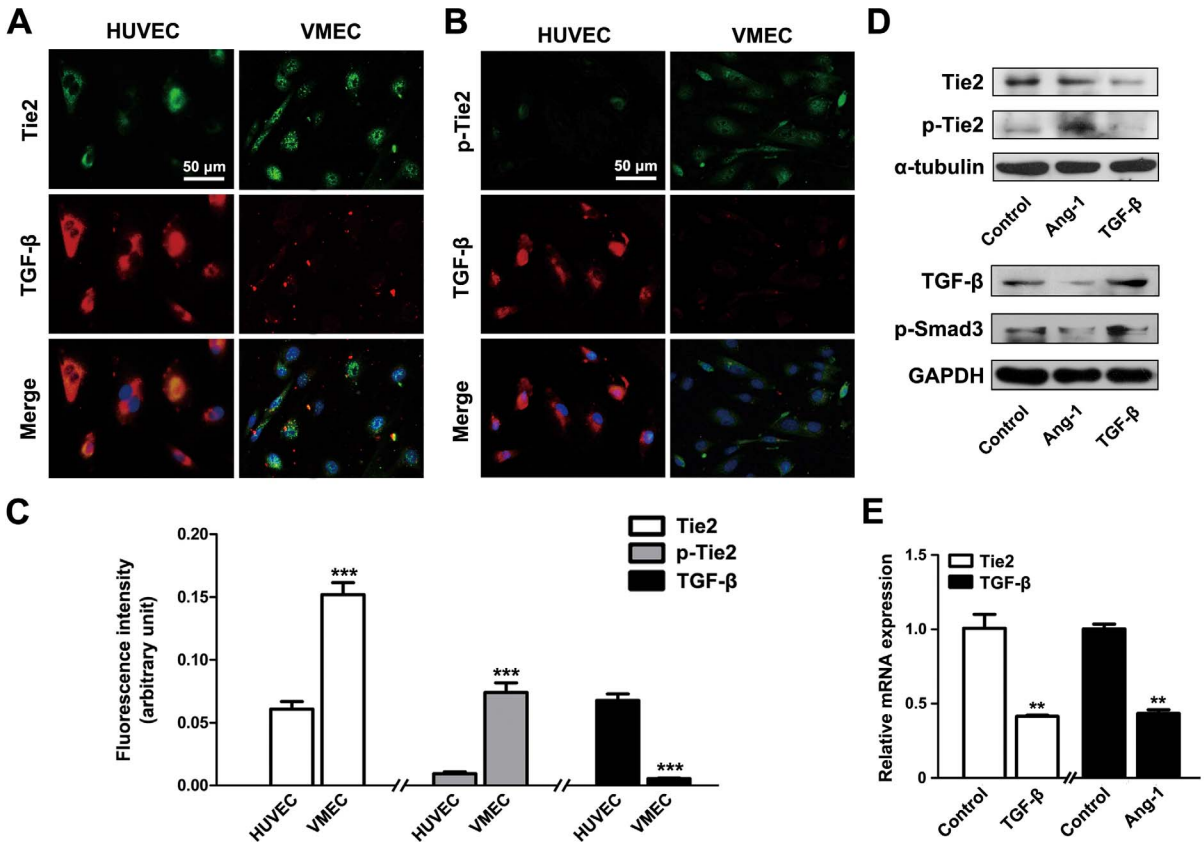

Figure 10 | Possible balancing effect between Tie2 and TGF-β in endothelial cells (ECs). (A, B) Tie2 and p-Tie2 upregulation and TGF-β downregulation are detected in venous malformation ECs (VMECs) when compared with HUVECs by double-immunofluorescence analysis of cells. Nuclei are counterstained with Hoechst. (C) The fluorescence intensities of Tie2 and p-Tie2 are significantly increased in VMECs when compared with HUVECs; the fluorescence intensity of TGF-β is decreased. Data are expressed as means ± SEM. ***, $P < 0.001$ versus HUVECs. (D) Expression levels of p-Tie2 and TGF-β/p-Smad3 in HUVECs are detected by western blot analysis after treatment with Tie2 agonist Ang-1 or recombinant TGF-β. The gels have been run under the same experimental conditions. The cropped gels/blots are used. (E) The mRNA expression levels of Tie2 and TGF-β in HUVECs are determined by real-time qPCR after treatment with recombinant TGF-β or Tie2 agonist Ang-1. Data are represented as the relative ratio to the control group without treatment (means ± SD for qPCR). **, $P < 0.01$ versus control group.

Table 2 | Primer sequences used for real-time quantitative PCR

Gene	Forward (5′-3′)	Reverse (5′-3′)
18s rRNA	CGGCTACCACATCCAAGGAA	GCTGGAATTACCGCGGCT
Tie2	AAGGGCCTAGAGCCTGAAAC	AGAAAGGCCAACAGCACAGT
TGF-β	GGGACTATCCACCTGCAAGA	CCTCCTTGGCGTAGTAGTCG
VE-cadherin	ACGGGATGACCAAGTACAGC	ACACACTTTGGGCTGGTAGG
N-cadherin	AGGGCCTTAAAGCTGCTGACA	TCATAGTCGAAGACTAAAAGGGAGTCATAT

1. Richter, G. T. & Friedman, A. B. Hemangiomas and vascular malformations: current theory and management. *Int J Pediatr* **2012**, 645678 (2012).
2. Tucci, F. M. *et al.* Head and neck vascular anomalies in children. *Int J Pediatr Otorhinolaryngol* **73 Suppl 1**, S71–6 (2009).
3. Wang, Y., Qi, F. & Gu, J. Endothelial cell culture of intramuscular venous malformation and its invasive behavior related to matrix metalloproteinase-9. *Plast Reconstr Surg* **123**, 1419–30 (2009).
4. Legiehn, G. M. & Heran, M. K. Venous malformations: classification, development, diagnosis, and interventional radiologic management. *Radiol Clin North Am* **46**, 545–97, vi (2008).
5. Cahill, A. M. & Nijs, E. L. Pediatric vascular malformations: pathophysiology, diagnosis, and the role of interventional radiology. *Cardiovasc Intervent Radiol* **34**, 691–704 (2011).
6. Gupta, A. & Kozakewich, H. Histopathology of vascular anomalies. *Clin Plast Surg* **38**, 31–44 (2011).
7. Hristov, N., Atanasov, Z., Zafirovski, G. & Mitrev, Z. Intramuscular cavernous hemangioma in the left soleus muscle: successful surgical treatment. *Interact Cardiovasc Thorac Surg* **13**, 521–2 (2011).
8. Dhupar, V., Yadav, S., Dhupar, A. & Akkara, F. Cavernous hemangioma--uncommon presentation in zygomatic bone. *J Craniofac Surg* **23**, 607–9 (2012).
9. Ramina, K., Ebner, F. H., Ernemann, U. & Tatagiba, M. Surgery of Cavernous Hemangioma of the Optic Nerve: Case Report and Review. *J Neurol Surg A Cent Eur Neurosurg* **74**, 265–70 (2013).
10. Sanghvi, D., Munshi, M., Kulkarni, B. & Kumar, A. Dorsal spinal epidural cavernous hemangioma. *J Craniovertebr Junction Spine* **1**, 122–5 (2010).
11. Buckmiller, L. M., Richter, G. T. & Suen, J. Y. Diagnosis and management of hemangiomas and vascular malformations of the head and neck. *Oral Dis* **16**, 405–18 (2010).
12. Morris, P. N. *et al.* Functional analysis of a mutant form of the receptor tyrosine kinase Tie2 causing venous malformations. *J Mol Med (Berl)* **83**, 58–63 (2005).
13. Valenzuela, D. M. *et al.* Angiopoietins 3 and 4: diverging gene counterparts in mice and humans. *Proc Natl Acad Sci U S A* **96**, 1904–9 (1999).
14. Thomas, M. & Augustin, H. G. The role of the Angiopoietins in vascular morphogenesis. *Angiogenesis* **12**, 125–37 (2009).
15. Wouters, V. *et al.* Hereditary cutaneomucosal venous malformations are caused by TIE2 mutations with widely variable hyper-phosphorylating effects. *Eur J Hum Genet* **18**, 414–20 (2010).
16. Vikkula, M. *et al.* Vascular dysmorphogenesis caused by an activating mutation in the receptor tyrosine kinase TIE2. *Cell* **87**, 1181–90 (1996).
17. Limaye, N. *et al.* Somatic mutations in angiopoietin receptor gene TEK cause solitary and multiple sporadic venous malformations. *Nat Genet* **41**, 118–24 (2009).
18. Blaschuk, O. W. & Devemy, E. Cadherins as novel targets for anti-cancer therapy. *Eur J Pharmacol* **625**, 195–8 (2009).
19. Derycke, L. *et al.* Soluble N-cadherin fragment promotes angiogenesis. *Clin Exp Metastasis* **23**, 187–201 (2006).
20. Huang, Y. H. *et al.* STAT1 activation by venous malformations mutant Tie2-R849W antagonizes VEGF-A-mediated angiogenic response partly via reduced bFGF production. *Angiogenesis* **16**, 207–22 (2013).
21. Gaengel, K., Genové, G., Armulik, A. & Betsholtz, C. Endothelial-mural cell signaling in vascular development and angiogenesis. *Arterioscler Thromb Vasc Biol* **29**, 630–8 (2009).
22. Dickson, M. C. *et al.* Defective haematopoiesis and vasculogenesis in transforming growth factor-beta 1 knock out mice. *Development* **121**, 1845–54 (1995).
23. Cao, R. *et al.* Angiogenic synergism, vascular stability and improvement of hind-limb ischemia by a combination of PDGF-BB and FGF-2. *Nat Med* **9**, 604–13 (2003).
24. Brouillard, P. & Vikkula, M. Genetic causes of vascular malformations. *Hum Mol Genet* **16 Spec No. 2**, R140–9 (2007).
25. Kontos, C. D. *et al.* Tyrosine 1101 of Tie2 is the major site of association of p85 and is required for activation of phosphatidylinositol 3-kinase and Akt. *Mol Cell Biol* **18**, 4131–40 (1998).
26. Chen, G. *et al.* Hypoxia-induced autophagy in endothelial cells: a double-edged sword in the progression of infantile haemangioma? *Cardiovasc Res* **98**, 437–48 (2013).
27. Sun, Z. J. *et al.* LMO2 promotes angiogenesis probably by up-regulation of bFGF in endothelial cells: an implication of its pathophysiological role in infantile haemangioma. *Histopathology* **57**, 622–32 (2010).
28. Zou, H. X., Jia, J., Zhang, W. F., Sun, Z. J. & Zhao, Y. F. Propranolol inhibits endothelial progenitor cell homing: a possible treatment mechanism of infantile hemangioma. *Cardiovasc Pathol* **22**, 203–10 (2013).
29. Chen, G. *et al.* Mammalian target of rapamycin regulates isoliquiritigenin-induced autophagic and apoptotic cell death in adenoid cystic carcinoma cells. *Apoptosis* **17**, 90–101 (2012).
30. Jia, J. *et al.* Epithelial mesenchymal transition is required for acquisition of anoikis resistance and metastatic potential in adenoid cystic carcinoma. *PLoS One* **7**, e51549 (2012).

Acknowledgments

This research was supported by the Doctoral Program Foundation of Higher Education of China (20130141120089), the Project funded by China Postdoctoral Science Foundation (2013M540607) and National Natural Science Foundation of China (81300895) to Dr. G. Chen; the Doctoral Program Foundation of Higher Education of China (20130141130006) and the National Natural Science Foundation of China (81170977, 81371159) to Prof. Y. F. Zhao.

Author contributions

G.C., J.G.R. and Y.F.Z. conceived and designed the project. J.G.R., F.Q.W., R.F.L. and J.Z. performed the experiments. G.C., W.Z., Y.F.S. and Y.F.Z. analyzed the data. G.C., J.G.R., W.Z. and Y.F.Z. wrote the paper. G.C. and J.G.R. contributed equally to the work. All of the authors read and approved the final manuscript.

Additional information

Funding sources: This research was supported by the Doctoral Program Foundation of Higher Education of China (20130141120089), the Project funded by China Postdoctoral Science Foundation (2013M540607) and National Natural Science Foundation of China (81300895) to Dr. G. Chen; the Doctoral Program Foundation of Higher Education of China (20130141130006) and the National Natural Science Foundation of China (81170977, 81371159) to Prof. Y. F. Zhao.

Competing financial interests: The authors declare no competing financial interests.

How to cite this article: Chen, G. *et al.* Disorganized vascular structures in sporadic venous malformations: a possible correlation with balancing effect between Tie2 and TGF-β. *Sci. Rep.* **4**, 5457; DOI:10.1038/srep05457 (2014).